

Design and Synthesis of Pyrazoline Inhibitors of SARS-CoV-2 NSP14

Elliott B. Smyth,* João P. Pisco, Kristian Birchall, Nicole S. Upfold, Arvind H. Patel, Richard Foster, and Jonathan M. Large*

Cite This: <https://doi.org/10.1021/acsmedchemlett.5c00155>

Read Online

ACCESS |



Metrics & More



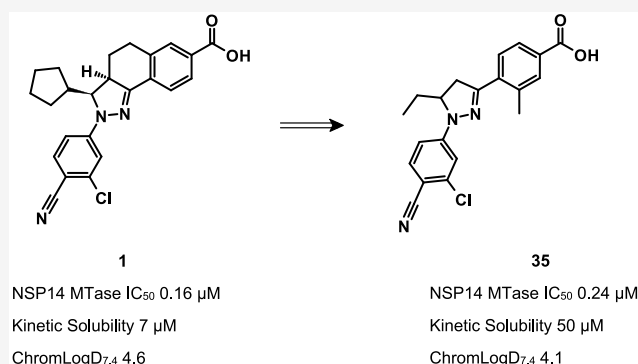
Article Recommendations



Supporting Information

ABSTRACT: Non-structural protein 14 (NSP14) is a key two-domain protein responsible for maintaining coronavirus replication fidelity, and in its absence reproduction is severely impacted. With the goal of identifying new inhibitors of SARS-CoV-2 NSP14, we selected a previously reported scaffold as an appropriate starting point. Medicinal chemistry exploration provided a series of trisubstituted pyrazolines as inhibitors of NSP14 methyltransferase (MTase) activity, with improved synthetic tractability and in a promising molecular property space. This led to compound **35** as a potent inhibitor of NSP14 MTase with a favorable *in vitro* ADMET profile, and antiviral activity against SARS-CoV-2 replication. We propose that **35** is a useful chemical probe which is well-positioned to further interrogate *in vitro* biology and for further optimization toward the treatment of human coronaviruses.

KEYWORDS: Ligands, Inhibition, Inhibitors, Molecules, Peptides and Proteins, SARS-CoV-2



Severe acute respiratory syndrome coronavirus-2 (SARS-CoV-2) is the seventh known coronavirus (CoV) to infect humans, and follows SARS-CoV and Middle East respiratory syndrome coronavirus (MERS-CoV) as viruses which frequently cause severe disease and death.¹ There remains a clear and unmet need for novel antiviral agents that are designed to specifically target CoVs. SARS-CoV, SARS-CoV-2 and MERS-CoV are all Betacoronaviruses (BetaCoV) and it is likely that some future zoonotic threats will fall within this viral genus. Moreover, an increase in globalization, climate change and deforestation has made the prospect of future pandemics more likely - pandemics may become more frequent, with viruses able to spread more rapidly.^{2,3} Therefore, there is a significant and growing focus on the development of therapeutics with pan-BetaCoV activity. This could be achieved by targeting a conserved BetaCoV mechanism or enhancing the activity of existing antiviral drugs. For example, many prior SARS-CoV-2 drug discovery efforts focused on well-characterized targets including chymotrypsin-like cysteine main protease (M^{pro}), a structurally well-characterized protein with diverse chemical starting points for inhibitor development.^{4,5}

Among other possible viral targets for therapeutic intervention, non-structural protein 14 (NSP14) is an essential CoV-specific protein responsible for maintaining replication fidelity and evasion of the immune response. SARS-CoV NSP14 is well characterized structurally and biochemically,⁶ and several examples of NSP14 inhibitors have been previously reported.⁷ However, the majority of these remain in preclinical drug discovery stages. NSP14 is a bifunctional protein,

comprising an N-terminal 3'-5' proofreading exoribonuclease (ExoN) domain and a C-terminal N7-guanine methyltransferase (MTase) domain. Mutational studies have shown the ExoN and MTase activities to be functionally independent, with the two domains separated by a flexible hinge region.⁸ In addition, NSP14 has been shown to be partly responsible for excessive inflammation following SARS-CoV-2 infection.⁹

The N7-methylation of the viral mRNA cap is essential for the synthesis of viral proteins and is a key event for viral infection.¹⁰ The N7-methyl guanosine cap structure is recognized by the eukaryotic translation initiation factor 4E and participates in the initiation of viral mRNA translation into proteins. NSP14 uses S-adenosyl methionine (SAM) as a methyl donor to methylate the N7 position of 5' guanine, generating S-adenosyl homocysteine (SAH) as a byproduct, an endogenous competitive inhibitor of SAM. This is a key step in constructing the cap that is essential for mRNA stability and translation in human cells.¹¹ Ogando et al. investigated the functional importance of conserved N7-MTase residues and identified two substitutions (R310A and F426A in SARS-CoV) which abrogated SARS-CoV viability, and one substitution

Received: March 20, 2025

Revised: August 13, 2025

Accepted: August 27, 2025

(H424A) which attenuated SARS-CoV, SARS-CoV-2, MERS-CoV, and MHV, suggesting that the N7-MTase function is critical for BetaCoV replication.¹⁰ However, finding selective inhibitors of MTase activity may be challenging due to the presence of methyltransferases across the human proteome.^{12–15}

Methyltransferases in general have been subjected to significant drug discovery efforts, likely due to their roles in numerous cellular processes, and have been thoroughly reviewed.¹⁶ Commonly, inhibitors fall into two categories. Nucleoside inhibitors of MTases, in common with SAM-like structures, often suffer from limited selectivity and poor absorption, distribution, metabolism, excretion and toxicity (ADMET) properties.¹⁷ In contrast, MTase inhibitors with non-nucleoside structures are often more selective, and typically have improved ADMET and pharmacokinetic (PK) properties.¹⁶ Screening against NSP14 MTase is well documented within the literature and a range of nucleoside^{18,19} and non-nucleoside inhibitors^{7,20–22} have been identified. Meyer and co-workers report high-throughput screening of NSP14 MTase using a MTase-Glo assay, and identified compounds with IC_{50} values less than 10 μ M.⁷ Hit selection and thorough optimization led to TDI-015051 with picomolar biochemical inhibition of NSP14 MTase. A second key approach utilized high-throughput screening of a 5000-compound library in a homologous time-resolved fluorescence (HTRF) assay, and identified a number of low micromolar inhibitors of NSP14 MTase, including a nonsteroidal mineralocorticoid antagonist, PF-03882845 (**1**, Figure 1).²⁰ Typically, the pan-MTase inhibitor sinefungin (**2**, Figure 1) is used as a positive control in screening campaigns.^{23–25}

In this work, we initially sought to validate previously reported inhibitors of NSP14 MTase in an NSP14 MTase-Glo assay,²⁶ with a goal to identify and prioritise chemotypes suitable for further design and optimization (Figures S1, S2;

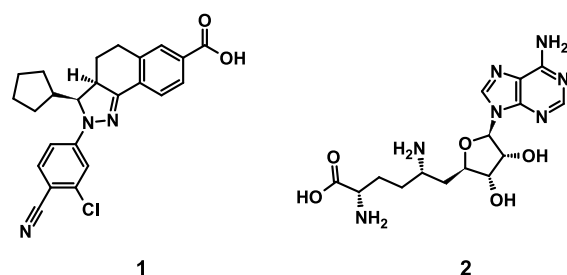


Figure 1. Examples of reported inhibitors of NSP14 MTase.²⁰

Table S1).^{20,21,27} Compound **1** emerged, displaying notable biochemical potency, with an IC_{50} of 0.16 μ M (in our hands, this was 10-fold more potent than previously reported). Compound **1** has been thoroughly characterized,^{28,29} and was previously in development for the treatment of diabetic nephropathy and hypertension. Molecular docking of **1** to an NSP14 MTase crystal structure (PDB: 5C8T³⁰) was used to investigate the putative binding mode and guide further compound design (Figure S3). The synthetic route to **1** and its analogues is well understood and requires four steps, including chiral separation by chiral supercritical fluid chromatography (SFC) to isolate the desired single enantiomer. Hence, we selected this molecule as the focus for further work.

We began by characterizing **1** and a small number of close analogues 3–6, prepared using routes adopted from Meyers et

al. (Scheme S1)^{28,29} in biochemical and ADMET assays, and observed that this tricyclic series suffered from poor kinetic solubility (Table 1). The inclusion of an acidic substituent appeared to be important for biochemical activity, as replacing the carboxylic acid (**4**) with a methyl ester (**3**) or removing it entirely (**5**) abolished activity. Moreover, the tricyclic fused-ring system did not lend itself to a rapid structure–activity relationship (SAR) assessment. To overcome these factors, we designed an alternative ‘ring-opened’ scaffold. Compound **7** was prepared following literature precedent,²⁸ and showed a significant improvement in kinetic solubility, though with a decrease in biochemical potency – which may be due to an entropic penalty for the ligand to adopt the bound conformation.³¹ A decrease in lipophilic ligand efficiency (LLE) was also observed as a result of the reduction in biochemical activity.

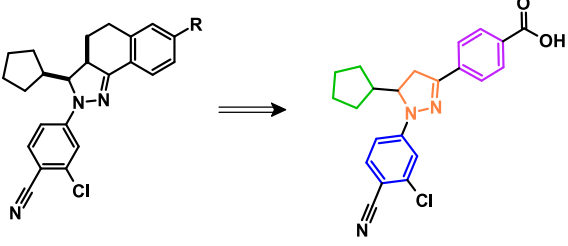
Although a significant loss in potency was observed, moving to a ring-opened aryl pyrazoline chemotype gave a simplified scaffold amenable to multiple synthetic approaches. Pyrazoline-containing molecules are commonly observed in drug discovery, for example in molecules with application in inflammation, oncology, and neurodegeneration settings.^{32–36} As a result, substituted pyrazolines are commonly accessed *via* a number of orthogonal routes using widely available starting materials which enable broad chemical exploration.

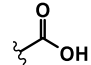
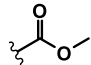
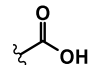
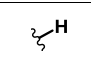
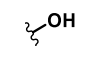
With a continuing focus on lipophilicity and solubility, we assessed whether a cyclopentyl group was required for the ring-opened series of compounds. Utilizing a linear synthetic route, an initial condensation of aryl hydrazines with α,β -unsaturated esters under basic conditions afforded key pyrazolinone intermediates. Subsequent chlorination was followed by coupling with aryl boronic acids or esters using standard Suzuki coupling conditions. Utilizing this or similar routes, where the required α,β -unsaturated esters were not commercially available, compounds 8–12 were prepared. In the alternative route, α,β -unsaturated ketones were prepared either by using an aldol procedure from a methyl ketone and the desired aldehyde, or *via* a 3-step process (Scheme S2).

Our initial SAR analysis indicated that the cyclopentyl group was not essential for inhibiting NSP14 MTase. Removing it completely (**8**), or replacing it with smaller methyl (**9**) or ethyl (**10**) groups gave improvements to physicochemical properties, particularly a significant reduction in $ChromLogD_{7.4}$ (Table 2). The methyl analogue **9** also showed no loss of biochemical activity and a 2.5-fold increase in kinetic solubility. This increase in potency was coupled with a pleasing sign of an improved LLE between **7** and **9** (0.7 vs 1.9). In contrast, larger, more lipophilic substituents, such as cyclohexyl (**12**), were not tolerated and resulted in a poorer profile.

In order to establish requirements in the southern aromatic ring, the pyrazoline core bearing a methyl group was maintained, as this gave the best balance of potency, physicochemical properties, and synthetic tractability. Key molecules 18–20 were prepared from unsaturated ester **13**, *via* intermediates 14–17 (Scheme 1), to assess the influence of the chlorine and nitrile substituents (Table 3). We found that both appeared to contribute to the potency of these molecules, particularly the chlorine substituent, which provided a ~10-fold increase in potency. However, this came at a detriment to solubility, as compound **9** (bearing both the chlorine and nitrile substituents) showed a reduction in solubility, which was restored when either or both were removed.

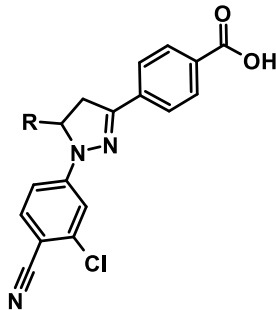
Table 1. Structures, NSP14 MTase Biochemical Activity, and Physicochemical Properties of 1 and 3–7 (Compound 7 is Coloured According to Each Component of the Molecule Subsequently Investigated; Northern Ring (Purple), Pyrazoline Core (Orange), Pyrazoline 3'-Substituent (Green) and Southern Ring (Blue))



Compound	R	pIC ₅₀	Kinetic Solubility (μM)	ChromLogD _{7.4}	LLE ^a
1		6.8	7	4.6	2.2
3		<4.0	<1	>6.4	-
4		6.5	<1	4.6	1.9
5		<4.0	<1	>6.4	-
6		5.3	8	>6.4	-
7	-	5.2	32	4.5	0.7

^aLLE = pIC₅₀ – ChromLogD_{7.4}.

Table 2. Structures, NSP14 MTase Biochemical Activity, and Physicochemical Properties of 7–12

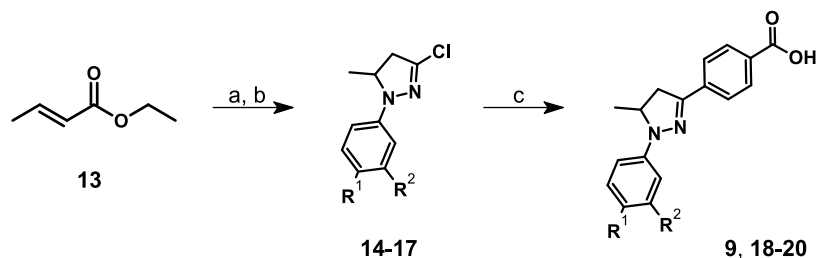


Compound	R	pIC ₅₀	Kinetic Solubility (μM)	ChromLogD _{7.4}	LLE ^a
7	CyPentyl	5.2	32	4.5	0.7
8	H	4.3	9	3.0	1.3
9	Me	5.3	86	3.4	1.9
10	Et	6.4	51	3.8	2.6
11	ⁱ Pr	5.5	48	3.9	1.6
12	CyHexyl	<4.0	36	5.1	-

^aLLE = pIC₅₀ – ChromLogD_{7.4}.

We turned to the second aryl ring to investigate whether alternative substitution patterns or heterocycles could be incorporated. Hence a further small set of compounds were prepared using a similar synthetic approach to that shown in Scheme 1. Moving the carboxylic acid from the 4'-position (as in 9) to the 3'-position (as in 21) maintained biochemical activity (Table 4). Though furan 22 gave a marked loss in inhibitory activity, the commonly employed isostere thiophene 23 increased potency and lipophilic efficiency.

One factor contributing to these substantial changes in activity could be a substituent vector effect. For 3'-substituted compound 21 and 4'-substituted compound 9 the angles are 120° and 180°, respectively. Similarly, furan 22 and thiophene 23 have different substitution angles, 125° and 148°, respectively.³⁷ Alternatively, the difference in activity could be due to the relative electron densities of each of the aromatic rings. Although thiophene 23 functioned as a suitable benzene ring isostere with improvements to biochemical activity and LLE, we chose not to pursue its further development. Substituted thiophenes are commonly oxidized by cytochrome P450 enzymes, leading to metabolites which cause toxic side effects.³⁸ Furthermore, we decided that adding a thiophene moiety would impede a rapid SAR study, because of the limited availability of commercially sourced substituted

Scheme 1. Route used to Synthesise Compounds 9 and 18–20^a

^aReagents and conditions: (a) aryl hydrazine, NaOEt, EtOH; (b) POCl₃, MeCN; (c) 4-carboxybenzeneboronic acid pinacol ester, Pd(PPh₃)₄, Na₂CO₃, H₂O, 1,4-dioxane or DME.

Table 3. NSP14 MTase Biochemical Activity and Physicochemical Properties of Compounds 9 and 18–20

Compound	R ¹	R ²	pIC ₅₀	Kinetic Solubility (μM)	ChromLogD _{7.4}	LLE ^a
9	CN	Cl	5.3	86	3.4	1.9
18	H	H	4.0	>200	3.1	0.9
19	CN	H	4.4	>200	2.7	1.7
20	H	Cl	5.1	>200	3.8	1.3

^aLLE = pIC₅₀ – ChromLogD_{7.4}.

thiophenes suitable for inclusion. Despite some improvement in solubility when moving to a 3'-substituted acid (**21**), a 4'-benzoic acid (as in **9**) was maintained in future designs.

To probe the requirement for the carboxylic acid, we prepared compounds bearing alternative acidic functional groups *via* the same chemical approach. Replacing the carboxylic acid with an amide (**24**) or sulfonamide (**25**)

abolished the activity (Table 5). In contrast, the more acidic acyl sulfonamides **26–27** showed low micromolar inhibition of NSP14 MTase, albeit with a significantly poorer kinetic solubility. Another well-known carboxylic acid isostere, tetrazole **28**, was prepared and retained a single-digit micromolar inhibition. Phenol **29** showed no biochemical activity and suggested a more acidic motif was required. These replacements of the carboxylic acid also led to expected increases in lipophilicity (except for **26**), and typically reduced kinetic solubility.

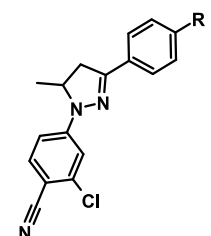
Finally, the impact of additional substitution to the northern ring was examined with a view to improving key molecular properties. It was hypothesized that adding an *ortho*-substituent to the northern ring may introduce a conformational 'twist' to this series of molecules, with potential for further increasing solubility. To probe this, compounds bearing 2'-substituents were designed and synthesized as before. Encouragingly, the addition of a 2'-methyl group (**30**) gave an improvement in solubility, and while similar levels of

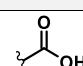
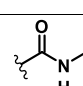
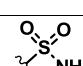
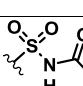
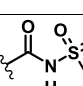
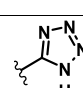
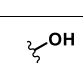
Table 4. Structures, NSP14 MTase Biochemical Activity, and Physicochemical Properties of 9, 21–23

Compound	R	pIC ₅₀	Kinetic Solubility (μM)	ChromLogD _{7.4}	LLE ^a
9		5.3	86	3.4	1.9
21		5.5	>200	3.2	2.3
22		4.2	>200	2.8	1.4
23		6.1	>200	3.2	2.9

^aLLE = pIC₅₀ – ChromLogD_{7.4}.

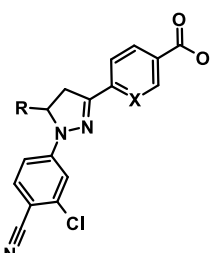
Table 5. Biochemical Activity and Physicochemical Properties of Compounds 9 and 24–29



Compound	R	pIC ₅₀	Kinetic Solubility (μM)	ChromLogD _{7.4}	LLE ^a
9		5.3	86	3.4	1.9
24		<4.0	<1	5.5	-
25		<4.0	<1	5.5	-
26		5.7	<1	3.3	2.4
27		5.7	7	3.6	2.1
28		5.2	20	3.8	1.4
29		<4.0	81	6.3	-

^aLLE = pIC₅₀ – ChromLogD_{7.4}.

Table 6. NSP14 MTase Biochemical Activity and Physicochemical Properties of Compounds 9, 10 and 30–35

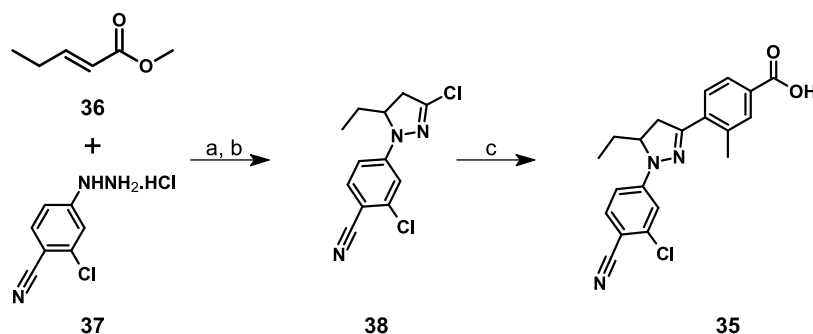


Compound	R	X	pIC ₅₀	Kinetic Solubility (μM)	ChromLogD _{7.4}	LLE ^a
9	Me	C–H	5.3	86	3.4	1.9
10	Et	C–H	6.4	51	3.8	2.6
30	Me	C–Me	5.8	151	3.5	2.3
31	Me	C–F	5.4	16	3.5	1.9
32	Me	C–OMe	4.7	162	3.5	1.2
33	Me	C–CN	5.0	46	3.4	1.7
34	Me	N	<4.0	>200	2.8	-
35	Et	C–Me	6.6	50	4.1	2.6

^aLLE = pIC₅₀ – ChromLogD_{7.4}.

potency were observed, this came with increased lipophilicity and resulted in a modest improvement to LLE (Table 6). Hence further 2'-substituents such as fluoro (31), methoxy

(32) and cyano (33) groups were prepared for further comparison. While a marked improvement in kinetic solubility was observed for methyl- and methoxy-containing compounds

Scheme 2. Synthesis of Compound 35^a

^aReagents and conditions: (a) NaOEt, EtOH; (b) POCl₃, MeCN; (c) 3-Methyl-4-(4,4,5,5-tetramethyl-1,3,2-dioxaborolan-2-yl)benzoic acid, Pd(PPh₃)₄, Na₂CO₃, H₂O, 1,4-dioxane or DME.

Table 7. Further *In Vitro* ADMET Characterization of Compounds 1 and 35

Compound	1	35
MLM CL _{int} (μL/mL/mg)	7.1	<5.0
HLM CL _{int} (μL/mL/mg)	<5.0	<5.0
Permeability (Caco-2)		
A-B P _{app} (10 ⁻⁶ cm/s)	6.0	9.7
B-A P _{app} (10 ⁻⁶ cm/s)	4.8	12.3
Efflux ratio	0.8	1.3
CTG [A549] EC ₅₀ (μM)	>50	>50

30 and 32, all other compounds had moderate solubility and did not maintain the biochemical activity shown by 30. A final adjustment to incorporate a 2'-pyridyl ring (34), which could also lower lipophilicity *via* additional polarity, showed no biochemical activity, which may be due to a larger change in dihedral angle between the two rings, causing a stable, but unfavorable conformation.

To combine previous observations, we reverted to an ethyl-substituted core (in 10) and installed the 2'-methyl group, resulting in compound 35 (Scheme 2). This promisingly showed an additive effect with respect to biochemical activity with potent inhibition of NSP14 MTase with a pIC₅₀ of 6.6. A

continued improvement in LLE was observed when compared to compound 9, indicating that the additional groups were efficiently contributing to biochemical activity.

We subsequently assessed compound 35 in *in vitro* ADMET assays, particularly to evaluate metabolic stability, permeability and cell toxicity, and compared these to compound 1 (Table 7). Good metabolic stability was observed in both microsomes and hepatocytes, with half-lives >60 min which were comparable to starting point 1. To probe the selectivity of this series, compounds 1 and 35 were assessed against a panel of 15 methyltransferase proteins (Figure S4). Satisfyingly, both compounds showed good selectivity with moderate inhibition of only two methyltransferases at 10 μM. Following this, compound 35 was profiled in a permeability assay in Caco-2 cells. Pleasingly, an improvement in permeability was observed, and compound 35 exhibited a Caco-2 P_{app} value of 9.7 × 10⁻⁶ cm/s, and neither compound 1 nor 35 showed significant efflux concerns. In order to assess for compound toxicity, a CellTiter-Glo (CTG) cell viability assay showed no cytotoxicity was observed for the selected compounds, with EC₅₀ values >50 μM in both cases. Hence, compound 35 possessed a well-balanced *in vitro* profile and prompted us to investigate its activity in a cellular assay.

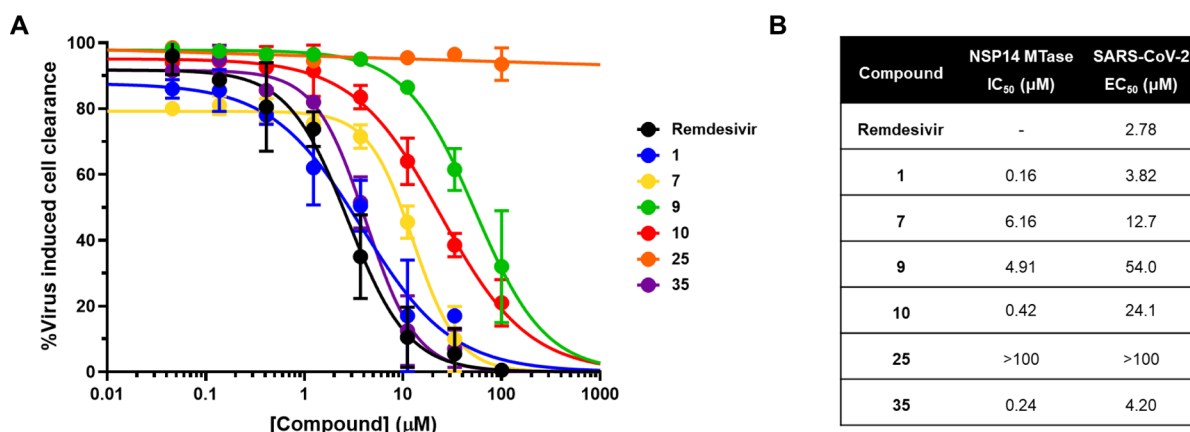


Figure 2. (A) Antiviral activity of NSP14 MTase inhibitors 1, 7, 9, 10, 25, and 35 against SARS-CoV-2. Calu3 cells were pretreated with a 3-fold dilution range of inhibitor or remdesivir and infected with SARS-CoV-2 B.1.617.2 at an MOI of 0.1 for 72 h. The percentage of viral-induced cell clearance or cytopathic effect (CPE) at each concentration was scored microscopically relative to the untreated infected and mock-infected control wells on each plate. Toxicity-induced cell clearance was observed for compounds 1, 7, and 35 only at 100 μM, therefore these points were excluded from the analysis and EC₅₀ calculations. Data are mean ± standard deviation from two independent biological experiments (*n* = 2). Individual points represent the mean of two technical duplicates per biological replicate. (B) Table showing comparison of NSP14 MTase biochemical activity and antiviral activity for remdesivir 1, 7, 9, 10, 25 and 35.

Compounds **1** and **35**, and a further set of representative inhibitors, were subsequently assessed in a viral infection assay (Figure 2, Figure S5, Table S2). Each compound was screened against the SARS-CoV-2 B.1.617.2 (Delta) variant in Calu3 cells. Viral-induced cell clearance in the presence of each serially diluted compound or remdesivir control³⁹ was scored microscopically, 3 days post infection. Both compounds **1** and **35** inhibited viral-induced cell clearance with EC₅₀ values in the low micromolar range, similar to remdesivir. Toxicity-induced clearance was observed only at a top concentration of 100 μ M for **1**, **7** and **35**. A dose-dependent response was observed for all compounds except **25**, which showed no effect up to 100 μ M and did not inhibit NSP14 in biochemical assays. Overall, *in vitro* biochemical activity correlated well with cellular assay results, with the most potent NSP14 inhibitors exhibiting the strongest antiviral effects. Notably, several low micromolar NSP14 MTase inhibitors displayed EC₅₀ values exceeding 20 μ M in cellular assays, indicating a >10-fold reduction in potency. A representative example is the matched pair **10** and **35**, for which similar biochemical potencies (IC₅₀ = 0.42 and 0.24 μ M, respectively), were accompanied by differentiated cellular activities (EC₅₀ = 24.1 and 4.20 μ M, respectively). This discrepancy may be attributed to a moderate increase in lipophilicity (ChromLogD_{7.4} = 3.8 and 4.1), potentially improving the cell permeability for compound **35**.

In conclusion, our study successfully identified and explored a series of potent NSP14 MTase inhibitors, with compound **35** emerging as a promisingly positioned key exemplar. Compound **35** not only demonstrated excellent biochemical inhibition of NSP14 MTase, but also exhibited a favorable ADMET profile, including good metabolic stability and low cytotoxicity. Its potent antiviral activity, comparable to remdesivir, further derisks the target and series as an approach against human coronaviruses. Interestingly, evidence from the literature had previously suggested that potent, cell permeable NSP14 MTase inhibitors might have no effect on viral replication in SARS-CoV-2.⁴⁰ Compound **35** exemplifies one of the first small molecule inhibitors of NSP14 MTase with antiviral activity. Hence, we have begun to investigate a series of potent inhibitors of NSP14, with excellent ADMET profiles, in an attractive position for further optimization for the treatment of human coronaviruses.

■ ASSOCIATED CONTENT

SI Supporting Information

The Supporting Information is available free of charge at <https://pubs.acs.org/doi/10.1021/acsmedchemlett.5c00155>.

Experimental procedures for the synthesis of Compound **4** and Compound **35**, characterization data for all compounds, and further details about the NSP14 MTase biochemical assay, methyltransferase selectivity panel, ADMET assays and viral replication assay (PDF)

■ AUTHOR INFORMATION

Corresponding Authors

Elliott B. Smyth – LifeArc, Stevenage SG1 2FX, U.K.; School of Chemistry, University of Leeds, Leeds LS2 9JT, U.K.; orcid.org/0009-0006-3717-2684; Email: elliott.smyth@lifearc.org

Jonathan M. Large – LifeArc, Stevenage SG1 2FX, U.K.; Email: jonathan.large@lifearc.org

Authors

João P. Pisco – LifeArc, Stevenage SG1 2FX, U.K.; orcid.org/0000-0001-6763-7354

Kristian Birchall – LifeArc, Stevenage SG1 2FX, U.K.

Nicole S. Upfold – MRC-University of Glasgow Centre for Virus Research, Glasgow G61 1QH, U.K.

Arvind H. Patel – MRC-University of Glasgow Centre for Virus Research, Glasgow G61 1QH, U.K.; CVR-CRUSH, MRC-University of Glasgow Centre for Virus Research, Glasgow G61 1QH, U.K.; orcid.org/0000-0003-4600-2047

Richard Foster – School of Chemistry, University of Leeds, Leeds LS2 9JT, U.K.; orcid.org/0000-0002-2361-3884

Complete contact information is available at:

<https://pubs.acs.org/10.1021/acsmedchemlett.5c00155>

Author Contributions

E.B.S. wrote the manuscript. E.B.S. designed and synthesized the compounds. R.F. and J.M.L. supervised the project and provided direction in compound design and project progression. J.P. provided *in vitro* biochemical assay results. K.B. provided computational chemistry support. N.S.U. and A.H.P. provided viral replication assay results. All authors contributed to, reviewed and approved the final manuscript.

Notes

The authors declare no competing financial interest.

No unexpected or unusually high safety hazards were encountered. All work with SARS-CoV-2 was carried out at biosafety containment level 3 (CL3).

■ ACKNOWLEDGMENTS

The authors thank LifeArc for funding and scientific resources. E.B.S. thanks the Royal Commission for the Exhibition of 1851 for funding *via* an Industrial Fellowship. E.B.S. thanks Dr Simon Osborne and Martin Ambler for their prior supervision and helpful discussions. We thank Dr Alice Webb and Magdy Mekdad for providing NSP14 protein, Dr Nathalie Bouloc and Dr Carmen Dregger for their analytical chemistry support, and Natasha Bury and Alfred Cross for providing cell toxicity data. A.H.P. acknowledges support from LifeArc COVID-19 award, and the MRC core award (MC_UU_00034/9).

■ ABBREVIATIONS

ADMET	absorption, distribution, metabolism, excretion and toxicity
BetaCoV	Betacoronavirus
ChromLogD _{7.4}	chromatographic method logD _{7.4}
CoV	coronavirus
CPE	cytopathic effect
CTG	CellTiter-Glo
Cy	cyclo
ExoN	exoribonuclease
HLM	human liver microsomes
LLE	lipophilic ligand efficiency
MERS-CoV	middle east respiratory syndrome coronavirus
MHV	mouse hepatitis virus
MLM	mouse liver microsomes
MOI	multiplicity of infection
MTase	methyltransferase
NAI	nucleoside analogue inhibitor
NSP14	non-structural protein 14
PK	pharmacokinetic

SAH	S-adenosyl homocysteine
SAM	S-adenosyl methionine
SAR	structure–activity relationship
SARS-CoV-2	Severe acute respiratory syndrome coronavirus-2
SFC	supercritical fluid chromatography

REFERENCES

- (1) Hu, T.; Liu, Y.; Zhao, M.; Zhuang, Q.; Xu, L.; He, Q. A comparison of COVID-19, SARS and MERS. *PeerJ*. **2020**, *8*, No. e9725.
- (2) Dobson, A. P.; Pimm, S. L.; Hannah, L.; Kaufman, L.; Ahumada, J. A.; Ando, A. W.; Bernstein, A.; Busch, J.; Daszak, P.; Engelmann, J.; Kinnaird, M. F.; Li, B. V.; Loch-Temzelides, T.; Lovejoy, T.; Nowak, K.; Roehrdanz, P. R.; Vale, M. M. Ecology and economics for pandemic prevention. *Science* **2020**, *369* (6502), 379–381.
- (3) Jones, K. E.; Patel, N. G.; Levy, M. A.; Storeygard, A.; Balk, D.; Gittleman, J. L.; Daszak, P. Global trends in emerging infectious diseases. *Nature* **2008**, *451* (7181), 990–3.
- (4) Owen, D. R.; Allerton, C. M. N.; Anderson, A. S.; Aschenbrenner, L.; Avery, M.; Berritt, S.; Boras, B.; Cardin, R. D.; Carlo, A.; Coffman, K. J.; Antonio, A.; Di, L.; Eng, H.; Ferre, R.; Gajiwala, K. S.; Gibson, S. A.; Greasley, S. E.; Hurst, B. L.; Kadar, E. P.; Kalgutkar, A. S.; Lee, J. C.; Lee, J.; Liu, W.; Mason, S. W.; Noell, S.; Novak, J. J.; Obach, R. S.; Ogilvie, K.; Patel, N. C.; Pettersson, M.; Rai, D. K.; Reese, M. R.; Sammons, M. F.; Sathish, J. G.; Singh, R. S. P.; Stepan, C. M.; Stewart, A. E.; Tuttle, J. B.; Updyke, L.; Verhoest, P. R.; Wei, L.; Yang, Q.; Zhu, Y. An oral SARS-CoV-2 M(pro) inhibitor clinical candidate for the treatment of COVID-19. *Science* **2021**, *374* (6575), 1586–1593.
- (5) Bobby, M. L.; Fearon, D.; Ferla, M.; Filep, M.; Koekemoer, L.; Robinson, M. C.; Chodera, J. D.; Lee, A. A.; London, N.; von Delft, A.; von Delft, F.; Achdout, H.; Aimon, A.; Alonzi, D. S.; Arbon, R.; Aschenbrenner, J. C.; Balcomb, B. H.; Bar-David, E.; Barr, H.; Ben-Shmuel, A.; Bennett, J.; Bilenko, V. A.; Borden, B.; Boulet, P.; Bowman, G. R.; Brewitz, L.; Brun, J.; Bvnbs, S.; Calmiano, M.; Carbery, A.; Carney, D. W.; Cattermole, E.; Chang, E.; Chernyshenko, E.; Clyde, A.; Coffland, J. E.; Cohen, G.; Cole, J. C.; Contini, A.; Cox, L.; Croll, T. L.; Cvitkovic, M.; De Jonghe, S.; Dias, A.; Donckers, K.; Dotson, D. L.; Douangamath, A.; Dubenstein, S.; Dudgeon, T.; Dunnett, L. E.; Eastman, P.; Erez, N.; Eyermann, C. J.; Fairhead, M.; Fate, G.; Fedorov, O.; Fernandes, R. S.; Ferrins, L.; Foster, R.; Foster, H.; Fraise, L.; Gabizon, R.; Garcia-Sastre, A.; Gawriljuk, V. O.; Gehrtz, P.; Gileadi, C.; Giroud, C.; Glass, W. G.; Glen, R. C.; Glinert, L.; Godoy, A. S.; Gorichko, M.; Gorrie-Stone, T.; Griffen, E. J.; Haneef, A.; Hassell Hart, S.; Heer, J.; Henry, M.; Hill, M.; Horrell, S.; Huang, Q. Y. J.; Huliak, V. D.; Hurley, M. F. D.; Israely, T.; Jajack, A.; Jansen, J.; Jnoff, E.; Jochmans, D.; John, T.; Kaminow, B.; Kang, L.; Kantsadi, A. L.; Kenny, P. W.; Kiappes, J. L.; Kinakh, S. O.; Kovar, B.; Krojer, T.; La, V. N. T.; Laghimi-Hahn, S.; Lefker, B. A.; Levy, H.; Lithgo, R. M.; Logvinenko, I. G.; Lukacik, P.; Macdonald, H. B.; MacLean, E. M.; Makower, L. L.; Malla, T. R.; Marples, P. G.; Matviiuk, T.; McCorkindale, W.; McGovern, B. L.; Melamed, S.; Melnykov, K. P.; Michurin, O.; Miesen, P.; Mikolajek, H.; Milne, B. F.; Minh, D.; Morris, A.; Morris, G. M.; Morwitzer, M. J.; Moustakas, D.; Mowbray, C. E.; Nakamura, A. M.; Neto, J. B.; Neyts, J.; Nguyen, L.; Noske, G. D.; Oleinikovas, V.; Oliva, G.; Overheul, G. J.; Owen, C. D.; Pai, R.; Pan, J.; Paran, N.; Payne, A. M.; Perry, B.; Pingle, M.; Pinjari, J.; Politi, B.; Powell, A.; Psenak, V.; Pulido, I.; Puni, R.; Rangel, V. L.; Reddi, R. N.; Rees, P.; Reid, S. P.; Reid, L.; Resnick, E.; Ripka, E. G.; Robinson, R. P.; Rodriguez-Guerra, J.; Rosales, R.; Rufa, D. A.; Saar, K.; Saikatendu, K. S.; Salah, E.; Schaller, D.; Scheen, J.; Schiffer, C. A.; Schofield, C. J.; Shafeev, M.; Shaikh, A.; Shaqra, A. M.; Shi, J.; Shurrush, K.; Singh, S.; Sittner, A.; Sjo, P.; Skyner, R.; Smalley, A.; Smeets, B.; Smilova, M. D.; Solmesky, L. J.; Spencer, J.; Strain-Damerell, C.; Swamy, V.; Tamir, H.; Taylor, J. C.; Tennant, R. E.; Thompson, W.; Thompson, A.; Tomasio, S.; Tomlinson, C. W. E.; Tsurupa, I. S.; Tumber, A.; Vakonakis, I.; van Rij, R. P.; Vangeel, L.; Varghese, F. S.; Vaschetto, M.; Vitner, E. B.; Voelz, V.; Volkamer, A.; Walsh, M. A.; Ward, W.; Weatherall, C.; Weiss, S.; White, K. M.; Wild, C. F.; Witt, K. D.; Wittmann, M.; Wright, N.; Yahalom-Ronen, Y.; Yilmaz, N. K.; Zaidmann, D.; Zhang, I.; Zidane, H.; Zitzmann, N.; Zvornicanin, S. N. Open science discovery of potent noncovalent SARS-CoV-2 main protease inhibitors. *Science* **2023**, *382* (6671), No. eabo7201.
- (6) Ogando, N. S.; Ferron, F.; Decroly, E.; Canard, B.; Posthuma, C. C.; Snijder, E. J. The Curious Case of the Nidovirus Exoribonuclease: Its Role in RNA Synthesis and Replication Fidelity. *Front Microbiol* **2019**, *10*, 1813.
- (7) Meyer, C.; Garzia, A.; Miller, M. W.; Huggins, D. J.; Myers, R. W.; Hoffmann, H. H.; Ashbrook, A. W.; Jannath, S. Y.; Liverton, N.; Kargman, S.; Zimmerman, M.; Nelson, A. M.; Sharma, V.; Dolgov, E.; Cangialosi, J.; Penalva-Lopez, S.; Alvarez, N.; Chang, C. W.; Oswal, N.; Gonzalez, I.; Rasheed, R.; Goldgrish, K.; Davis, J. A.; Ramos-Espiritu, L.; Menezes, M. R.; Larson, C.; Nitsche, J.; Ganichkin, O.; Alwaseem, H.; Molina, H.; Steinbacher, S.; Glickman, J. F.; Perlin, D. S.; Rice, C. M.; Meinke, P. T.; Tuschl, T. Small-molecule inhibition of SARS-CoV-2 NSP14 RNA cap methyltransferase. *Nature* **2025**, *637* (8048), 1178–1185.
- (8) Ferron, F.; Subissi, L.; Silveira De Moraes, A. T.; Le, N. T. T.; Sevajol, M.; Gluais, L.; Decroly, E.; Vonnrhein, C.; Bricogne, G.; Canard, B.; Imbert, I. Structural and molecular basis of mismatch correction and ribavirin excision from coronavirus RNA. *Proc. Natl. Acad. Sci. U. S. A.* **2018**, *115* (2), E162–E171.
- (9) Duan, T.; Xing, C.; Chu, J.; Deng, X.; Du, Y.; Liu, X.; Hu, Y.; Qian, C.; Yin, B.; Wang, H. Y.; Wang, R. F. ACE2-dependent and -independent SARS-CoV-2 entries dictate viral replication and inflammatory response during infection. *Nat. Cell Biol.* **2024**, *26* (4), 628–644.
- (10) Ogando, N. S.; El Kazzi, P.; Zevenhoven-Dobbe, J. C.; Bontes, B. W.; Decombe, A.; Posthuma, C. C.; Thiel, V.; Canard, B.; Ferron, F.; Decroly, E.; Snijder, E. J. Structure-function analysis of the nsp14 N7-guanine methyltransferase reveals an essential role in Betacoronavirus replication. *Proc. Natl. Acad. Sci. U. S. A.* **2021**, *118* (49), No. e2108709118.
- (11) Katahira, J.; Ohmae, T.; Yasugi, M.; Sasaki, R.; Itoh, Y.; Kohda, T.; Hieda, M.; Yokota Hirai, M.; Okamoto, T.; Miyamoto, Y. Nsp14 of SARS-CoV-2 inhibits mRNA processing and nuclear export by targeting the nuclear cap-binding complex. *Nucleic Acids Res.* **2023**, *51* (14), 7602–7618.
- (12) Aouadi, W.; Eydoux, C.; Coutard, B.; Martin, B.; Debar, F.; Vasseur, J. J.; Contreras, J. M.; Morice, C.; Querat, G.; Jung, M. L.; Canard, B.; Guillemot, J. C.; Decroly, E. Toward the identification of viral cap-methyltransferase inhibitors by fluorescence screening assay. *Antiviral Res.* **2017**, *144*, 330–339.
- (13) Sun, Y.; Wang, Z.; Tao, J.; Wang, Y.; Wu, A.; Yang, Z.; Wang, K.; Shi, L.; Chen, Y.; Guo, D. Yeast-based assays for the high-throughput screening of inhibitors of coronavirus RNA cap guanine-N7-methyltransferase. *Antiviral Res.* **2014**, *104*, 156–64.
- (14) Case, J. B.; Ashbrook, A. W.; Dermody, T. S.; Denison, M. R. Mutagenesis of S-Adenosyl-L-Methionine-Binding Residues in Coronavirus nsp14 N7-Methyltransferase Demonstrates Differing Requirements for Genome Translation and Resistance to Innate Immunity. *J. Virol* **2016**, *90* (16), 7248–7256.
- (15) Silhan, J.; Klima, M.; Otava, T.; Skvara, P.; Chalupska, D.; Chalupsky, K.; Kozic, J.; Nencka, R.; Boura, E. Discovery and structural characterization of monkeypox virus methyltransferase VP39 inhibitors reveal similarities to SARS-CoV-2 nsp14 methyltransferase. *Nat. Commun.* **2023**, *14* (1), 2259.
- (16) Talukdar, A.; Mukherjee, A.; Bhattacharya, D. Fascinating Transformation of SAM-Competitive Protein Methyltransferase Inhibitors from Nucleoside Analogues to Non-Nucleoside Analogues. *J. Med. Chem.* **2022**, *65* (3), 1662–1684.
- (17) Tsesmetzis, N.; Paulin, C. B. J.; Rudd, S. G.; Herold, N. Nucleobase and Nucleoside Analogues: Resistance and Re-Sensitisation at the Level of Pharmacokinetics, Pharmacodynamics and Metabolism. *Cancers* **2018**, *10* (7), 240.

- (18) Ahmed-Belkacem, R.; Troussier, J.; Delpal, A.; Canard, B.; Vasseur, J. J.; Decroly, E.; Debart, F. N-Arylsulfonamide-based adenosine analogues to target RNA cap N7-methyltransferase nsp14 of SARS-CoV-2. *RSC Med. Chem.* **2024**, *15* (3), 839–847.
- (19) Ahmed-Belkacem, R.; Hausdorff, M.; Delpal, A.; Sutto-Ortiz, P.; Colmant, A. M. G.; Touret, F.; Ogando, N. S.; Snijder, E. J.; Canard, B.; Coutard, B.; Vasseur, J. J.; Decroly, E.; Debart, F. Potent Inhibition of SARS-CoV-2 nsp14 N7-Methyltransferase by Sulfonamide-Based Bisubstrate Analogues. *J. Med. Chem.* **2022**, *65* (8), 6231–6249.
- (20) Basu, S.; Mak, T.; Ulferts, R.; Wu, M.; Deegan, T.; Fujisawa, R.; Tan, K. W.; Lim, C. T.; Basier, C.; Canal, B.; Curran, J. F.; Drury, L. S.; McClure, A. W.; Roberts, E. L.; Weissmann, F.; Zeisner, T. U.; Beale, R.; Cowling, V. H.; Howell, M.; Labib, K.; Diffley, J. F. X. Identifying SARS-CoV-2 antiviral compounds by screening for small molecule inhibitors of Nsp14 RNA cap methyltransferase. *Biochem. J.* **2021**, *478* (13), 2481–2497.
- (21) Kasprzyk, R.; Spiewla, T. J.; Smietanski, M.; Golojuch, S.; Vangeel, L.; De Jonghe, S.; Jochmans, D.; Neyts, J.; Kowalska, J.; Jemielity, J. Identification and evaluation of potential SARS-CoV-2 antiviral agents targeting mRNA cap guanine N7-Methyltransferase. *Antiviral Res.* **2021**, *193* (1872–9096 (Electronic)), No. 105142.
- (22) Samrat, S. K.; Bashir, Q.; Zhang, R.; Huang, Y.; Liu, Y.; Wu, X.; Brown, T.; Wang, W.; Zheng, Y. G.; Zhang, Q. Y.; Chen, Y.; Li, Z.; Li, H. A universal fluorescence polarization high throughput screening assay to target the SAM-binding sites of SARS-CoV-2 and other viral methyltransferases. *Emerg Microbes Infect* **2023**, *12* (1), No. 2204164.
- (23) Bobileva, O.; Bobrovs, R.; Kanepe, I.; Patetko, L.; Kalnins, G.; Sisovs, M.; Bula, A. L.; Gri Nberga, S.; Boroduskis, M. R.; Ramata-Stunda, A.; Rostoks, N.; Jirgensons, A.; Ta Rs, K.; Jaudzems, K. Potent SARS-CoV-2 mRNA Cap Methyltransferase Inhibitors by Bioisosteric Replacement of Methionine in SAM Cosubstrate. *ACS Med. Chem. Lett.* **2021**, *12* (7), 1102–1107.
- (24) Devkota, K.; Schapira, M.; Perveen, S.; Khalili Yazdi, A.; Li, F.; Chau, I.; Ghiabi, P.; Hajian, T.; Loppnau, P.; Bolotokova, A.; Satchell, K. J. F.; Wang, K.; Li, D.; Liu, J.; Smil, D.; Luo, M.; Jin, J.; Fish, P. V.; Brown, P. J.; Vedadi, M. Probing the SAM Binding Site of SARS-CoV-2 Nsp14 In Vitro Using SAM Competitive Inhibitors Guides Developing Selective Bisubstrate Inhibitors. *SLAS Discov* **2021**, *26* (9), 1200–1211.
- (25) Otava, T.; Sala, M.; Li, F.; Fanfrik, J.; Devkota, K.; Perveen, S.; Chau, I.; Pakarian, P.; Hobza, P.; Vedadi, M.; Boura, E.; Nencka, R. The Structure-Based Design of SARS-CoV-2 nsp14 Methyltransferase Ligands Yields Nanomolar Inhibitors. *ACS Infect Dis* **2021**, *7* (8), 2214–2220.
- (26) Hsiao, K.; Zegzouti, H.; Goueli, S. High throughput bioluminescent assay to characterize and monitor the activity of SARS-CoV-2 methyltransferases. *PLoS One* **2022**, *17* (11), No. e0274343.
- (27) Pearson, L. A.; Green, C. J.; Lin, P.; Petit, A. P.; Gray, D. W.; Cowling, V. H.; Fordyce, E. A. F. Development of a High-Throughput Screening Assay to Identify Inhibitors of the SARS-CoV-2 Guanine-N7-Methyltransferase Using RapidFire Mass Spectrometry. *SLAS Discov* **2021**, *26* (6), 749–756.
- (28) Meyers, M. J.; Arhancet, G. B.; Hockerman, S. L.; Chen, X.; Long, S. A.; Mahoney, M. W.; Rico, J. R.; Garland, D. J.; Blinn, J. R.; Collins, J. T.; Yang, S.; Huang, H. C.; McGee, K. F.; Wendling, J. M.; Dietz, J. D.; Payne, M. A.; Homer, B. L.; Heron, M. I.; Reitz, D. B.; Hu, X. Discovery of (3S,3aR)-2-(3-chloro-4-cyanophenyl)-3-cyclopentyl-3,3a,4,5-tetrahydro-2H-benzo[g] indazole-7-carboxylic acid (PF-3882845), an orally efficacious mineralocorticoid receptor (MR) antagonist for hypertension and nephropathy. *J. Med. Chem.* **2010**, *53* (16), 5979–6002.
- (29) Meyers, M. J.; Arhancet, G. B.; Chen, X.; Hockerman, S. L.; Long, S. A.; Mahoney, M. W.; Reitz, D. B.; Rico, J. G. Pyrazoline Compounds as Mineralocorticoid Receptor Antagonists. WO2008/053300, 2008.
- (30) Ma, Y.; Wu, L.; Shaw, N.; Gao, Y.; Wang, J.; Sun, Y.; Lou, Z.; Yan, L.; Zhang, R.; Rao, Z. Structural basis and functional analysis of the SARS coronavirus nsp14-nsp10 complex. *Proc. Natl. Acad. Sci. U. S. A.* **2015**, *112* (30), 9436–41.
- (31) Fang, Z.; Song, Y.; Zhan, P.; Zhang, Q.; Liu, X. Conformational restriction: an effective tactic in 'follow-on'-based drug discovery. *Future Med. Chem.* **2014**, *6* (8), 885–901.
- (32) Ahsan, M. J.; Ali, A.; Ali, A.; Thiriveedhi, A.; Bakht, M. A.; Yusuf, M.; Salahuddin; Afzal, O.; Altamimi, A. S. A. Pyrazoline Containing Compounds as Therapeutic Targets for Neurodegenerative Disorders. *ACS Omega* **2022**, *7* (43), 38207–38245.
- (33) Abou-Zied, H. A.; Beshr, E. A. M.; Hayallah, A. M.; Abdel-Aziz, M. Emerging insights into pyrazoline motifs: A comprehensive exploration of biological mechanisms and prospects for future advancements. *J. Mol. Struct.* **2024**, *1296*, No. 136807.
- (34) Haider, K.; Shafeeqe, M.; Yahya, S.; Yar, M. S. A comprehensive review on pyrazoline based heterocyclic hybrids as potent anticancer agents. *European Journal of Medicinal Chemistry Reports* **2022**, *5*, No. 100042.
- (35) Mantzanidou, M.; Pontiki, E.; Hadjipavlou-Litina, D. Pyrazoles and Pyrazolines as Anti-Inflammatory Agents. *Molecules [Online]* **2021**, *26*, 3439.
- (36) Alex, J. M.; Kumar, R. 4,5-Dihydro-1H-pyrazole: an indispensable scaffold. *J. Enzyme Inhib Med. Chem.* **2014**, *29* (3), 427–42.
- (37) Yang, J.; Lutz, M.; Grzech, A.; Mulder, F. M.; Dingemans, T. J. Copper-based coordination polymers from thiophene and furan dicarboxylates with high isosteric heats of hydrogen adsorption. *CrystEngComm* **2014**, *16* (23), 5121–5127.
- (38) Jaladanki, C. K.; Taxak, N.; Varikoti, R. A.; Bharatam, P. V. Toxicity Originating from Thiophene Containing Drugs: Exploring the Mechanism using Quantum Chemical Methods. *Chem. Res. Toxicol.* **2015**, *28* (12), 2364–76.
- (39) Schooley, R. T.; Carlin, A. F.; Beadle, J. R.; Valiaeva, N.; Zhang, X. Q.; Clark, A. E.; McMillan, R. E.; Leibel, S. L.; McVicar, R. N.; Xie, J.; Garretson, A. F.; Smith, V. I.; Murphy, J.; Hostetler, K. Y. Rethinking Remdesivir: Synthesis, Antiviral Activity, and Pharmacokinetics of Oral Lipid Prodrugs. *Antimicrob. Agents Chemother.* **2021**, *65* (10), No. e0115521.
- (40) Stefek, M.; Chalupska, D.; Chalupsky, K.; Zgarbova, M.; Dvorakova, A.; Krafcikova, P.; Li, A. S. M.; Sala, M.; Dejmek, M.; Otava, T.; Chaloupecka, E.; Kozak, J.; Kozic, J.; Vedadi, M.; Weber, J.; Mertlikova-Kaiserova, H.; Nencka, R. Rational Design of Highly Potent SARS-CoV-2 nsp14 Methyltransferase Inhibitors. *ACS Omega* **2023**, *8* (30), 27410–27418.